NON-STOP INTEGRAL FLOW IN LATERAL GAP DISTANCE LATTICE MODEL

Abstract

The role of non-stop integral flow is studied in a lattice model by assuming the lateral gap among the lattice sites. The proposed model is investigated theoretically as well as numerically. In theoretical evaluation, we derived the stableness criterion and provided the relationship among sensitivity and other parameters. It's far located that similarly to attention of the gap space, the non-stop time of flow reduces the congestion and the unstable region more reinforced via increasing the driver's memory time step.

Keywords: Integral flow, lateral gap, lattice model.

Authors

Vikash Siwach
Department of Mathematics and Statistics
CCS HAU
Haryana, Hisar, India
vikash@hau.ac.in

Poonam Redhu
Department of Mathematics
MDU
Rohtak, India
poonamr.maths@mdurohtak.ac.in

I. INTRODUCTION

To expose the traffic problems, including the intrinsic mechanisms of traffic congestion, commuting delay, traffic accidents, and energy consumption, the modeling of traffic flow has attracted a widespread interest of researchers in recent years. Most of the traffic techniques especially recognize the reproducing of the flow-density-velocity relationship and the phase transition of traffic flow from congested region to free flow region involving various factors of traffic [1, 2, 3, 4, 5, 6, 7]. Also, in order to reveal the actual traffic conditions, a few research studies have been added to suppress the traffic congestion. These days, the lattice hydrodynamic model which was firstly proposed by Nagatani [8], stimulates a huge interest of many researchers.

As we know, road conditions have a crucial role in traffic flow. Drivers tend to be more cautious and slow down when faced with obstacles on the road, such as restricted lanes, sharp curves, and rough road surfaces. Poor road conditions are a major cause of traffic jams. In this direction, car-following traffic flow models were proposed through [9, 10, 11] with the aid of assuming that vehicles travel in the center of the lane which can be stimulated directly by the only in front or behind and no passing is permitted on a single lane highway. By inspiring from Refs. [9, 10, 11], the impact of lateral gap has been also studied in lattice model [12] and it is determined that lateral separation performs a critical role in stabilizing the traffic flows in lattice fashions.

In real traffic, driver usually observe at the following in addition to the previous vehicles at some point of driving on road. To deal with these phenomena, many lattice models [13, 14, 15, 16, 17, 18, 19, 20, 21, 22] had been found within the literature. Currently, to show the role of historical traffic information, Wang and Ge [23] proposed a lattice model via accounting the "backward looking" and "flow integral effect" and it is observed that the stable region enhances efficiently with consideration of these factors. Motivated by this, Peng et al. [24] studied the flux difference memory integral effect in two-lane lattice version and it's far encountered that lane changing performs a vital function in stabilizing traffic congestion. Vehicle continuous memory is useful in traffic modelling, and the effect is amplified in non-lane-based lattice models. However, the lateral separation distance of consecutive autos has not been examined in the driver's continuous memory integral lattice model.

In section 2, we explore the lateral separations gap between two consecutive autos and offer a lateral-gap-distance lattice model while considering the effect of flow memory integral. In Section 3, the model's stability condition is established using linear stability theory. The numerical simulation is then completed in order to verify the analytic results, and the conclusion is stated in the concluding part.

II. PROPOSED MODEL

The lattice version of continuum model through considering the concept of car-following model is

$$\partial_t s_i + s_0(s_i v_i - s_{i-1} v_{i-1}) = 0, \tag{1}$$

With the given flow evolution equation at site i

$$\partial_t (s_i v_i) = a[s_0 v(s_{i+1}) - s_i v_i]. \tag{2}$$

Where $a = 1/\tau$ is the sensitivity; s_0 is the average density; V(.) is the optimal velocity function; s_i and v_i denote the density and velocity at site i at time t, respectively. Furthermore, to include the lateral separation distance, Peng et al. [12] proposed a lattice hydrodynamic model as follows

$$s_i(t+\tau) - s_i(t) + \tau s_0(s_i v_i - s_{i-1} v_{i-1}) = 0 \tag{3}$$

$$s_i(t+\tau)v_i(t+\tau) = s_0 V(s_{i+1}, s_{i+2}) + \omega G(\triangle Q_{i,i+1}, \triangle Q_{i,i+2}) \tag{4}$$

Where ω is the reactive coefficient to the function G(.), $\triangle Q_{i,i+1} = s_{i+1}v_{i+1} - s_i v_i$, and $\triangle Q_{i,i+2} = s_{i+2}v_{i+2} - s_i v_i$ are the relative flows among site i & i+1 and i & i+2, respectively. It's far observed that the free region enhances with an increase in the lateral separation distance of lane width, and consequently, this element plays an important role in stabilizing the traffic flow.

As we all know, a driver frequently observes traffic relevant data at time t and decides to change the vehicle's speed at a later time; nevertheless, this movement can produce a delay that influences traffic. In this course, Gupta and Redhu [26] presented a hydrodynamics model for detecting relative flux for a two-lane system with a fixed delay and explored the effects of driver expectation on traffic flow. However, it is clear that the effect of continual memory has a greater impact on traffic flow than the fixed delay time, and this has been examined in many traffic flow models [23, 27]. In the literature, we studied that road width performs an essential role in stabilizing traffic congestion, and it will become more effective if the driver could have relative records of continuous memory. But, the effect of non-stop memory integral has not been studied until now.

Here, we are offering a lattice model by accounting for persistent prior flux knowledge in terms of integration between the time [t −τ0, t] and the new evolution is

$$s_i(t+\tau)v_i(t+\tau) = s_0[V(s_{i+1}, s_{i+2})] + \omega \int_{t-\tau_0}^{\cdot} H(\triangle Q_{i,i+1}(s), \triangle Q_{i,i+2}(s))ds \tag{5}$$

Where τ0 represents the historical integral time, ω is the corresponding coefficient, G(.) is given by

$$H(\triangle Q_{i,i+1}(s), \triangle Q_{i,i+2}(s)) = (1-\gamma_i)\triangle Q_{i,i+1}(s) + \gamma_i \triangle Q_{i,i+2}(s) \tag{6}$$

and

$$V(s_{i+1}, s_{i+2}) = V[(1-\gamma_i)s_{i+1} + \gamma_i s_{i+2}] \tag{7}$$

Where $\gamma_i = \frac{LS_i}{LS_{max}}$ is lateral separation distance, LS_i is the lateral separation distance of between sites i and i+1 and LS_{max} is its maximum lateral distance. The term R tt−τ0

$G(\triangle Q_{i,i+1}(s), \triangle Q_{i,i+2}(s))ds$ represents the continuous flux difference information. The modified velocity function for non-lane-based model is

$$V(s_{i+1}, s_{i+2}) = \frac{v_{max}}{2}\left\{tanh\left[\frac{1}{(1-\gamma_i)s_{i+1} + \gamma_i s_{i+2}} - \frac{1}{s_c}\right] + tanh\left(\frac{1}{s_c}\right)\right\} \tag{8}$$

From Equations. (1) and (5) and eliminating vi, the equation of density is obtained as

$$s_i(t+2\tau) - s_i(t+\tau) + \tau s^2_0[V(s_{i+1}, s_{i+2}) - V(s_i, s_{i+1})] + \tau\omega[(1-\gamma_i)(-s_{i+1}(t) +$$
$$s_{i+1}(t-\tau_0)) + s_i(t) - s_i(t-\tau_0)) + \gamma_i(s_{j+2}(t) + s_{j+2}(t-\tau_0) + s_{j+1}(t) - s_{j+1}(t-\tau_0))] = 0 \tag{9}$$

III. LINEAR STABILITY ANALYSIS

To look the effect of memory flow integral in the proposed model, we suppose the resulting steady-state solution of the homogeneous traffic flow is as follows:

$$s_i(t) = s_0, \quad V_i(t) = V(s_0). \tag{10}$$

where s_0 and $V(s_0)$ represent the state of uniform traffic flow. Let $\eta_i(t)$ be a small perturbation to the steady-state density on site i. Then,
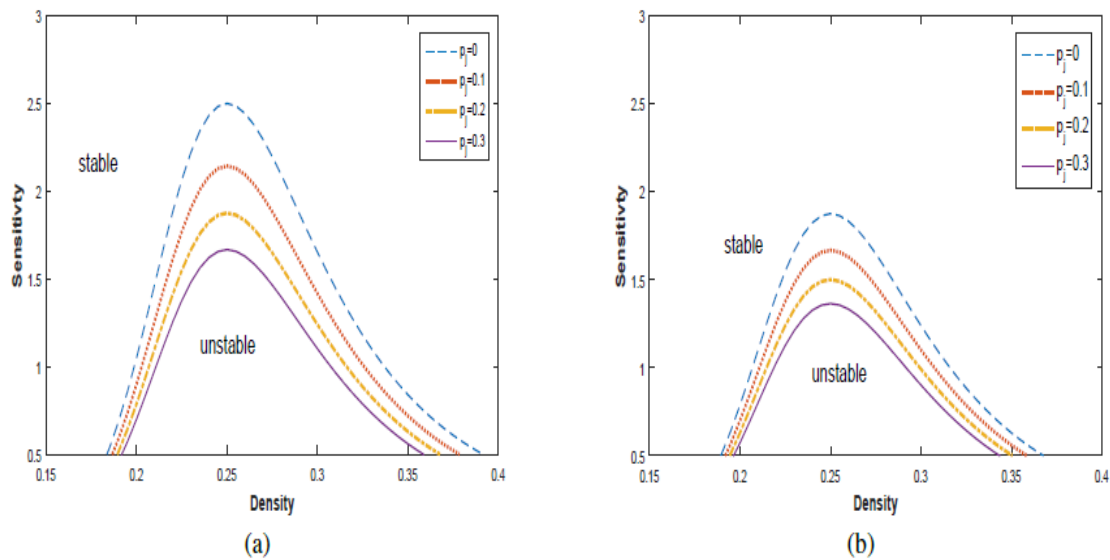
$$s_i(t) = s_0 + \eta_i(t). \tag{11}$$

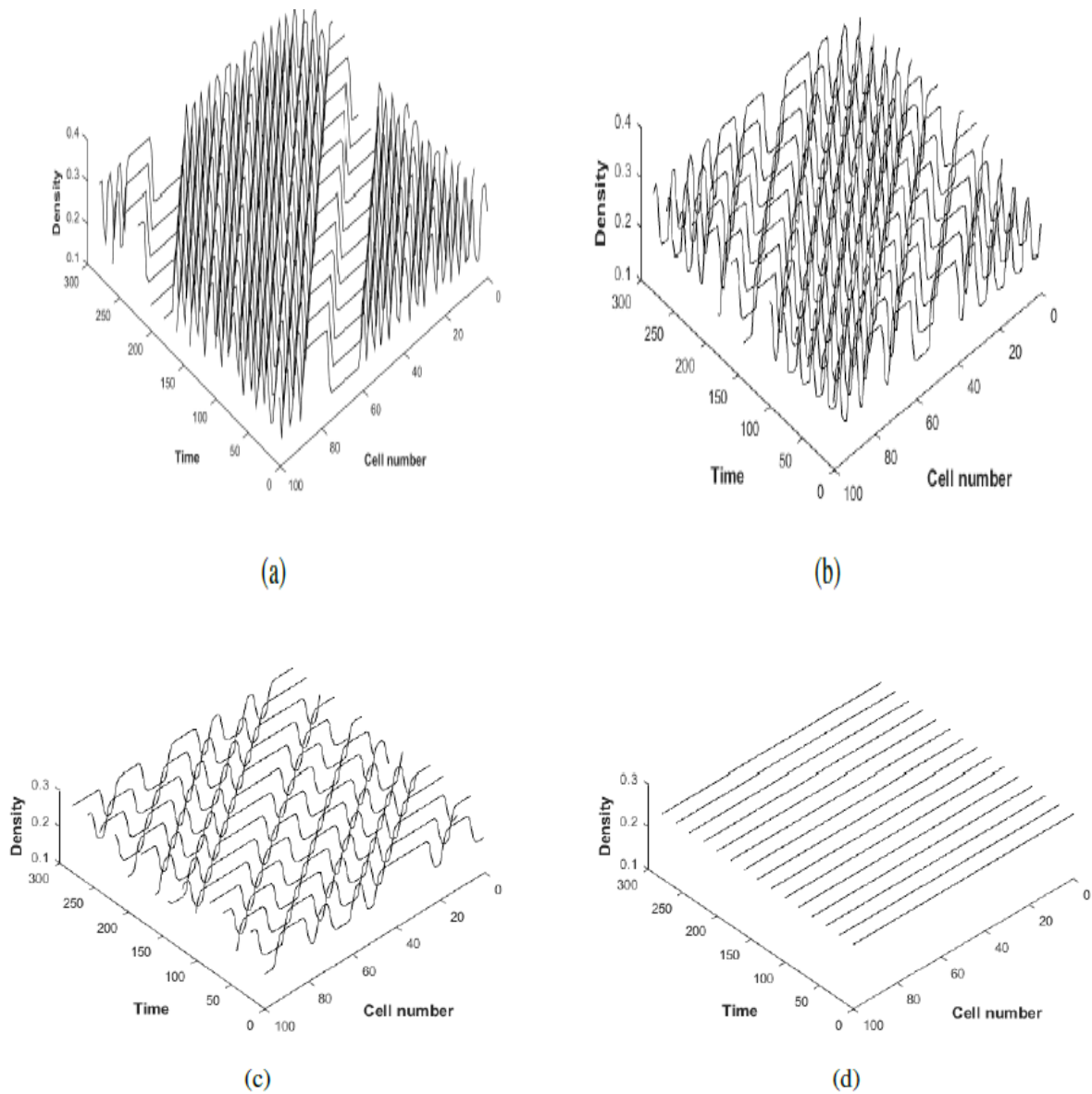**Figure 1:** Parameterized phase diagram (s,a), for (a) ω = 0.1 and (b) ω = 0.3, respectively.

Figure 2: Space time evolution after time t = 20000 for (a) $\gamma_i = 0$, (b) $\gamma_i = 0.1$, (c) $\gamma_i = 0.2$, and (d) $\gamma_i = 0.3$, for ω = 0.1.

Putting this perturbed density profile into Eq. (9) and linearizing it, we get

$$\eta_i(t+2\tau)-\eta_i(t+\tau)+\tau s^2{}_0 V'(s_0)[(1-\gamma_i)(\eta_{i+1}-\eta_i(t))+\gamma_i\,(\eta_{i+2}-\eta_{i+1})]+\tau\omega[(1-\gamma_i)(-\eta_{i+1}(t)$$
$$+\eta_{i+1}(t-\tau_0)+\eta_i(t)-\eta_i(t-\tau_0))+\gamma_i\,(\eta_{i+2}(t)+\eta_{i+2}(t-\tau_0)+\eta_{i+1}(t)-\eta_{i+1}(t-\tau_0))]=0 \qquad (12)$$
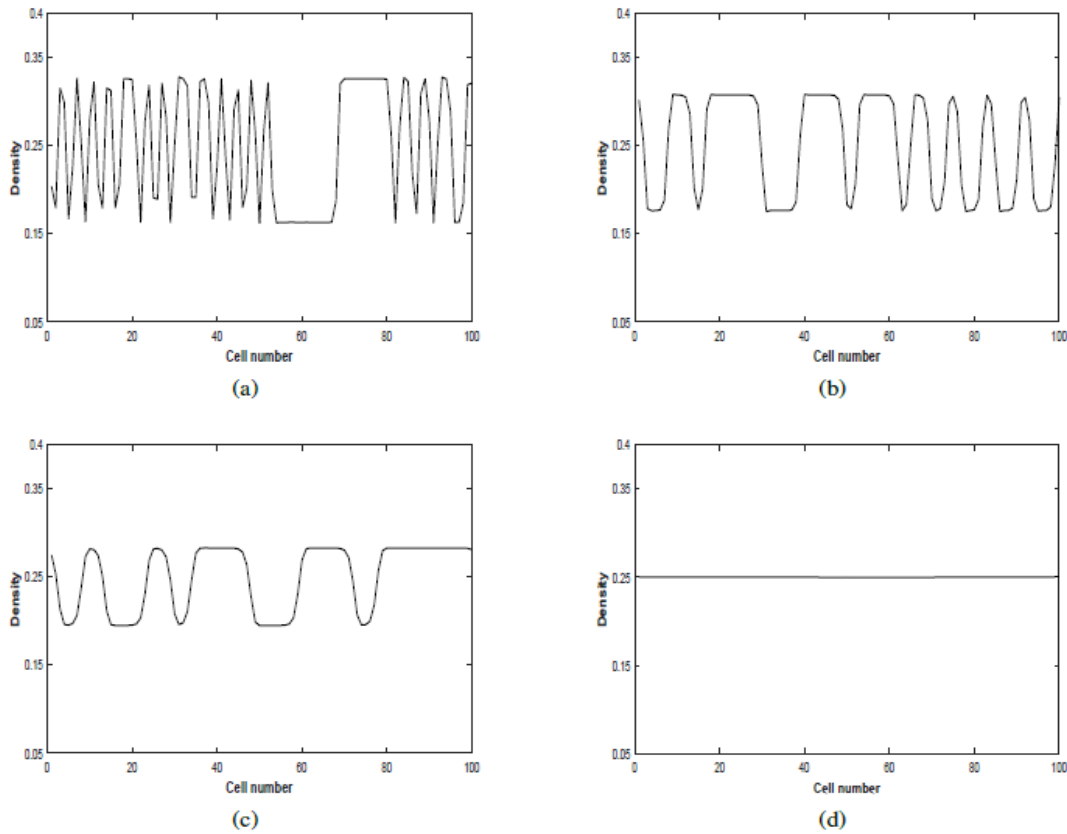
Figure 3: Density profile at time t = 20300 for (a) $\gamma_i = 0$, (b) $\gamma_i = 0.1$, (c) $\gamma_i = 0.2$, and (d) $\gamma_i = 0.3$, respectively for $\omega = 0.1$.

Substituting $\eta_i(t) = \exp(\imath kl + zt)$ in Eq. (12), we obtain

$$e^{2\tau z} - e^{\tau z} + \tau s_0^2 V'(s_0)[(1-\gamma_j)(e^{\imath k} - 1) + \gamma_i(e^{\imath k - \tau_0 z} - e^{-\tau_0 z})] + \tau \omega[(1-\gamma_i)$$
$$(-e^{\imath k} + e^{\imath k - \tau_0 z} + 1 - e^{\tau_0 z}) + \gamma_i(e^{2\imath k} + e^{2\imath k - \tau_0 z} + e^{\imath k} - e^{\imath k - \tau_0 z})] = 0. \qquad (13)$$

Inserting $z = z_1(ik) + z_2(ik)^2 ...$ into Eq. (13), we will obtain the first-order and second-order terms of the coefficient ik and $(ik)^2$, respectively, we get

$$z_1 = -s_0^2 \, V'(s_0), \qquad (14)$$

$$z_2 = -\frac{3\tau z_1^2}{2} - \frac{s_0^2 V'(s_0)}{2}(1 + 2\gamma_i) + \omega\tau_0. \qquad (15)$$

When z_2 is less than zero, long-wavelength waves lead to instability in the uniform steady-state flow. Conversely, when z_2 is greater than zero, the uniform flow attains stability. As a results, the "stability condition" for the "steady-state" is

$$\tau = -\frac{1 + 2\gamma_i + 2\omega\tau_0}{3s_0^2 V'(s_0)}. \qquad (16)$$

The instability requirement for homogeneous traffic flow is as follows:

$$\tau > -\frac{1+2\gamma_i+2\omega\tau_0}{3s_0^2 V'(s_0)}. \tag{17}$$

For $\omega = 0$, and $\gamma_i = 0$, the above instability criteria (Eq. 17) will match with Nagatani's [8] model.

Figure 1 shows the phase diagram in the parameter space (s, a) for different values of γ_i. The figure in Fig. 1(a) unmistakably demonstrates that as the value of γ_i increases while keeping ω at 0.1, the amplitude of the neutral stability curves declines. A further increment in the value of ω, the region corresponding to stability widens with a change in the value of γ_i. On comparing the results for $\omega = 01$. and $\omega = 0.3$, t is determined that as the value of increases, so does the stable region, which is further enhanced as the value of γ_i increases. If we compare our result with the Peng et al. [25] model for $\omega = 0.1$ it is concluded that the stable region is larger in the proposed model, which shows that the continuous delay of the flow integral plays an effective role in stabilizing the traffic flow.

IV. NUMERICAL SIMULATION

In this portion, we applied periodic boundary conditions to run a numerical simulation to validate the theoretical conclusions. The following are the beginning conditions:

$$s_i(1)=s_i(0)=\begin{cases} s_{0;} & i \neq \frac{N}{2}, \frac{N}{2}+1 \\ s_0 - B; & i = \frac{N}{2} \\ s_0 - B; & i = \frac{N}{2}+1 \end{cases}$$

where, B is the initial disturbance, N is the total number of sites taken as 100 and other parameters are set as follows: B = 0.1, $\tau = 1/a$.
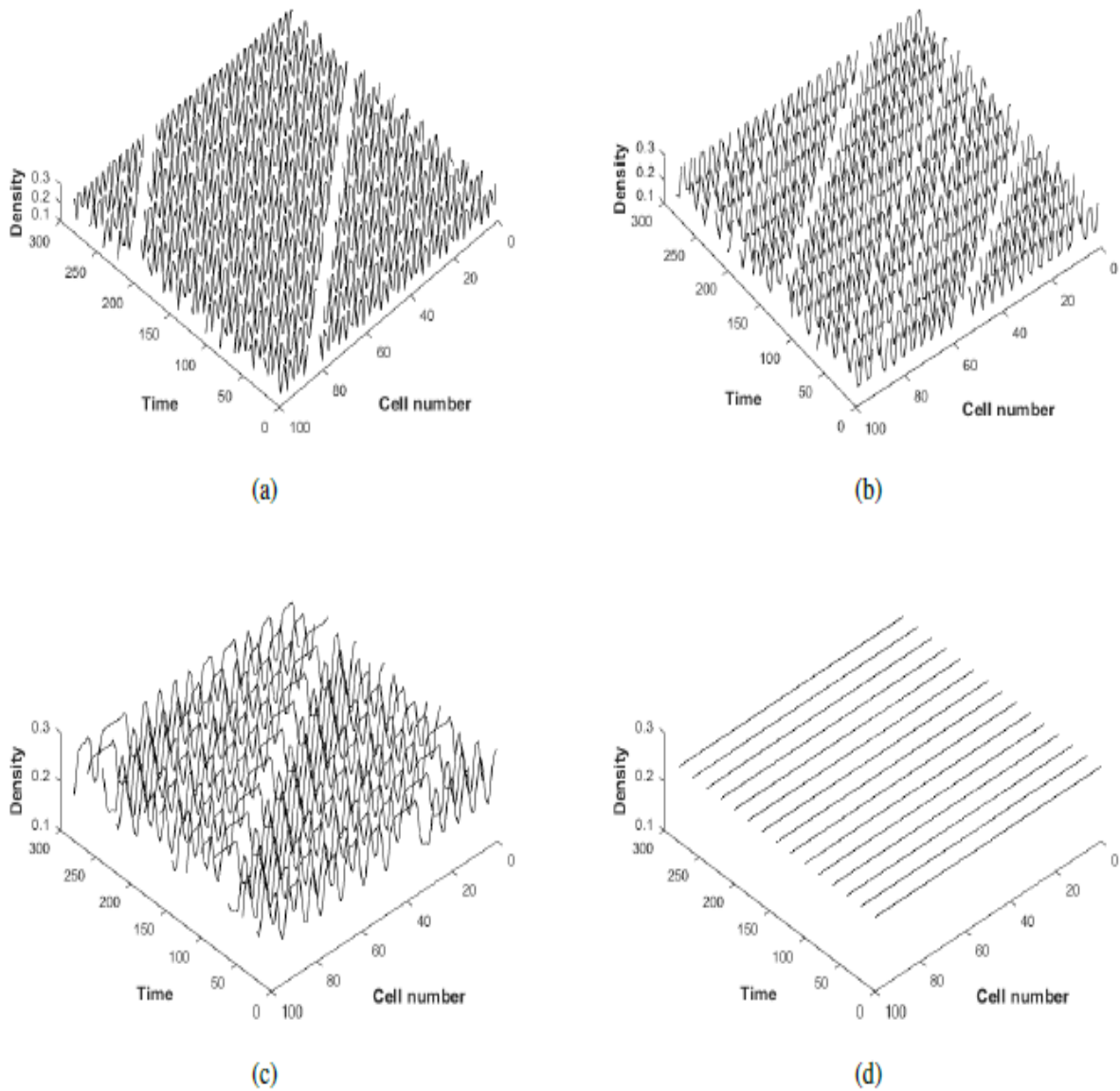
Figure 4: Space time evolution after time t = 20000 for (a) $\gamma_i = 0$, (b) $\gamma_i = 0.1$, (c) $\gamma_i = 0.2$, and (d) $\gamma_i = 0.3$, when $\omega = 0.3$.

The dynamical changes of density vibration at time t = 20000s−20300s for numerous values of γ_i when a = 1.7 and $\omega = 0.1$ are shown in Fig. 2. The traffic congestion develops in the unstable zone which appears in "kinkantikink" of waves that arise at each position and travel in the backward fashion over time, as seen in Figs. 2(a)-(c). We enter the stable region when $\gamma_i = 0.3$, and the density waves dissipate, and the traffic flow gets a bit more uniform.
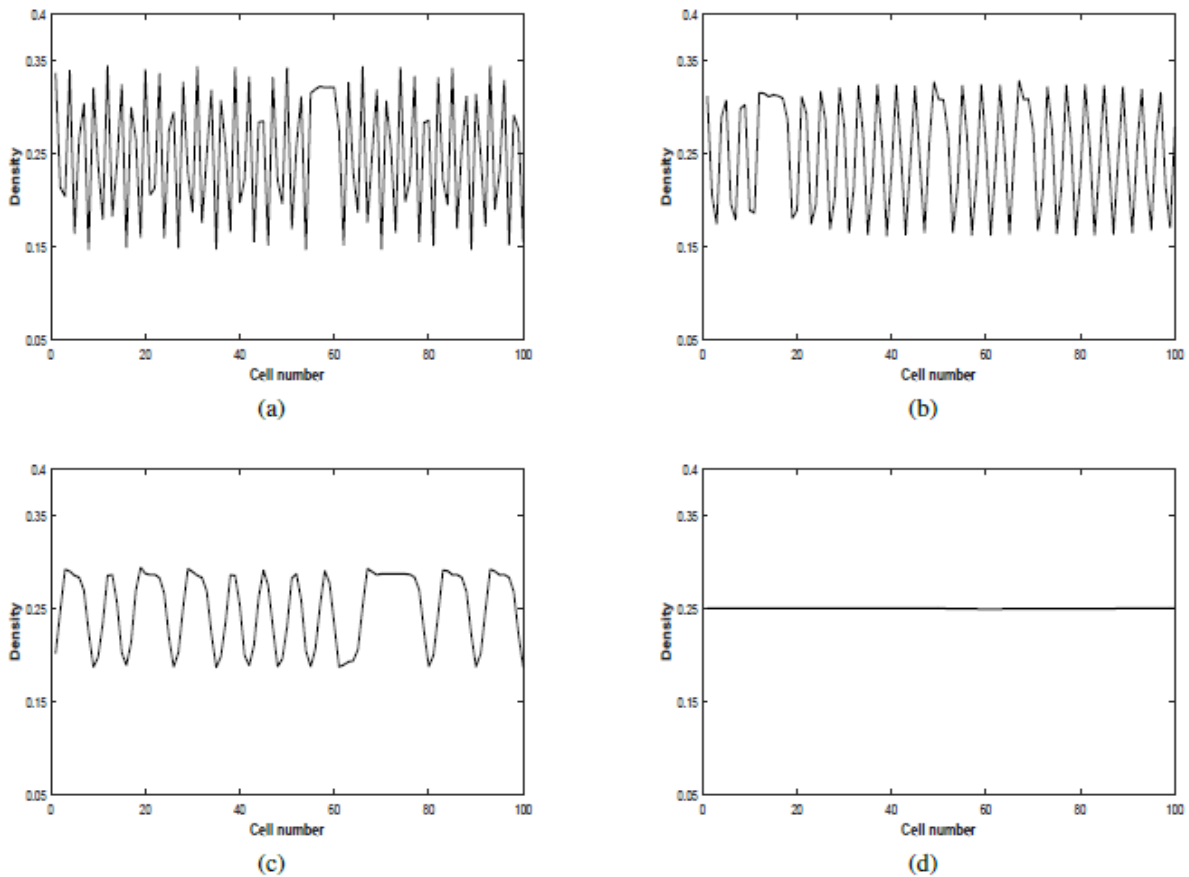
Figure 5: Density profile at time t = 20300 for (a) $\gamma_i = 0$, (b) $\gamma_i = 0.1$, (c) $\gamma_i = 0.2$, and (d) $\gamma_i = 0.3$, respectively for ω = 0.3.

The density profile after a suitably long time t = 20300 is shown in Fig.3, which corresponds to the panel in Fig.2. The intensity of the kink-antikink density wave diminishes as the value of γ_i grows, and the flow becomes uniform at $\gamma_i = 0.3$. Figure 4 depicts the spatiotemporal pattern of density waves at time t = 20000s−20300s for various values of γ_i when a = 1.52 and ω = 0.3. Figure 5 reveals the density profile at t = 20300, which aligns to the panel of Fig.4. In the unstable zone, the initial disturbance transforms into density motions, as seen in Fig.4 (a)-(c), and these fade away in the free flow region, as shown in Fig. 4(d). The deviation occurs around the critical density in the crowded zone, as illustrated in Figs.5(a)-(c), and this deviation disappears in Fig. 5(d). Thus, we may assert that the lateral separation distance significantly contributes to the preservation of a stable traffic flow.

When the results for ω = 0.1 and ω = 0.3 are compared, it is concluded that the information of continuous memory integral plays a vital role in traffic flow theory, and its influence is more pronounced in non-lane-based lattice
hydrodynamic models.

V. CONCLUSION

A non-lane-based lattice traffic flow model is proposed with consideration of the continuous flow integral effect. Through linear analysis, the condition of stability is derived

to analyze the traffic congestion region. Theoretical results are cross-checked by running a simulation with periodic boundary conditions. Our research aimed to understand the consequences of altering lateral separation distance while keeping ω constant on traffic flow. The outcome of our study indicates that the coefficient of flow integral effect contributes to the stabilization of traffic flow and should be integrated into traffic flow modeling.

DECLARATION OF CONFLICTS INTEREST

There are no conflicts of interest with this work disclosed by the authors.

DATA AVAILABILITY STATEMENT

There are no related data with this manuscript.

REFERENCES

[1] Tang, T.Q., Li, C.Y., Wu, Y.H., Huang, H.J., Impact of the honk effect on the stability of traffic flow, Phys. A, 390, 3362-3368 (2011)
[2] Tang, T.Q., Li, C.Y., Huang, H.J., A new car-following model with the consideration of the driver's forecast effect, Phys. Lett. A, 374,
[3] 3951-3956 (2010)
[4] Tang, T.Q., Wang, Y.P., Yang, X.B., Wu, Y.H., A new car-following model accounting for varying road condition, Nonlinear Dyn., 70, 1397-
[5] 1405 (2012)
[6] Daganzo, C.F., Requiem for second-order fluid approximations of traffic flow, Trans. Res. Part B Methodol., 29, 277-286 (1995)
[7] Berg, P., Mason, A., Woods, A., Continuum approach to car-following models, Phys. Rev. E, 61, 1056 (2000)
[8] Jiang, R., Wu, Q.S., Zhu, Z.J., A new continuum model for traffic flow and numerical tests, Trans. Res. Part B Methodol., 36, 405-419 (2002)
[9] Gupta, A.K., Redhu, P., Analyses of the driver's anticipation effect in a new lattice hydrodynamic traffic flow model with passing, Nonlinear
[10] Dyn., 76, 1001-1011 (2014)
[11] Nagatani, T., Modified kdv equation for jamming transition in the continuum models of traffic, Phys. A, 261, 599-607 (1998)
[12] Gunay, B., Car following theory with lateral discomfort, Transp. Res. B 41, 722,(2007)
[13] Jin, S., Wang, D.H., Tao, P.F., Li, P.F., Non-lane-based full velocity difference car following model, Phys. A, 389, 4654-4662 (2010)
[14] Li, Y., Zhang, L., Peeta, S., Pan, H., Zheng, T., Li, Y. and He, X., Non-lane-discipline-based car-following model considering the effects of
[15] two-sided lateral gaps, Nonlinear Dyn., 80, 227-238 (2015)
[16] Peng, G.H., Cai, X.H., Cao, B.F., Liu, C.Q., Non-lane-based lattice hydrodynamic model of traffic flow considering the lateral effects of the
[17] lane width, Phys. Lett. A, 375, 2823-2827 (2011)
[18] Nagatani, T., Chaotic jam and phase transition in traffic flow with passing, Phys. Rev. E, 60, 1535 (1999)
[19] Ge, H.X., Cheng, R.J., The backward looking effect in the lattice hydrodynamic model, Phys. A, 387, 6952-6958 (2008)
[20] Peng, G.H., Cai, X.H., Liu, C.Q. and Cao, B.F., A new lattice model of traffic flow with the consideration of the driver's forecast effects. Phys.
[21] Lett. A, 375, 2153-2157 (2011)
[22] Peng, G., Nie, F., Cao, B. and Liu, C., A driver's memory lattice model of traffic flow and its numerical simulation. Nonlinear Dyn., 67(3),
[23] 1811-1815 (2012)
[24] Tian, J.F., Yuan, Z.Z., Jia, B., Li, M.H. and Jiang, G.J., The stabilization effect of the density difference in the modified lattice hydrodynamic

[25] model of traffic flow. Phys. A, 391(19), 4476-4482 (2012)

[26] Peng, G., A new lattice model of two-lane traffic flow with the consideration of optimal current difference. Commun. Nonlinear Sci. Numer.

[27] Simul., 18(3), 559-566 (2013)

[28] Ge, H.X., Zheng, P.J., Lo, S.M. and Cheng, R.J., TDGL equation in lattice hydrodynamic model considering driver's physical delay. Nonlinear

[29] Dyn., 76(1), 441-445 (2014)

[30] Redhu, P., Gupta, A.K., Jamming transitions and the effect of interruption probability in a lattice traffic flow model with passing, Phys. A, 421,

[31] 249-260 (2015)

[32] Redhu, P. and Gupta, A.K., Effect of forward looking sites on a multi-phase lattice hydrodynamic model. Phys. A, 445, 150-160 (2016)

[33] Redhu, P. and Siwach, V., An extended lattice model accounting for traffic jerk. Phys. A, 492, 1473-1480 (2018)

[34] Wang, Q. and Ge, H., An improved lattice hydrodynamic model accounting for the effect of "backward looking" and flow integral. Phys. A,

[35] 513, 438-446 (2019)

[36] Peng, G., Yang, S., Zhao, H. and Qing, L., The flux difference memory integral effect on two-lane stability in the lattice hydrodynamic model,

[37] Int. J. Mod. Phys. C, 29, 1850083 (2018)

[38] Peng, G.H., Cai, X.H., Cao, B.F. and Liu, C.Q., Non-lane-based lattice hydrodynamic model of traffic flow considering the lateral effects of

[39] the lane width, Phys. Let. A, 375, 2823-2827 (2011)

[40] Gupta, A.K. and Redhu, P., Analyses of driver's anticipation effect in sensing relative flux in a new lattice model for two-lane traffic system,

[41] Phys. A, 392(22), 5622-5632 (2013)

[42] Cao, B.G., A new car-following model considering driver's sensory memory, Phys. A, 427, 218-225 (2015)